Advances in Engineering Research : Possibilities and Challenges
ISSN Print: 3079-5192
ISSN Online: 3079-5206
https://doi.org/10.63313/AERpc.9049

Experimental Study on Dynamic Modulation Op-timization of Micro-Hole Morphology in Wa-ter-Assisted Laser Drilling

Fan Liu[1.2.3]. Shufeng Sun[1.2.3.*]. Junbao Li[1.2.3]
[1]Discipline lnnovation and Wisdom Introduction Base of High-end Laser Intelligent Manufacturing Technology and Equipment, Qingdao University of Technology, Qingdao 266525, China
[2]Shandong Provincial Key Laboratory of Laser Green Intelligent Manufacturing Technology, Qingdao University of Technology, Qingdao. 266525, China
[3]Qingdao University of Technology, Qingdao. 266525, China
Email: sunshufeng@qut.edu.cn

How to cite this paper: Liu, F., Sun, S. F., & Li, J. B. (2025). Experimental Study on Dynamic Modulation Optimization of Micro-Hole Morphology in Water-Assisted Laser Drilling. Advances in Engineering Research: Possibilities and Challenges, 2(2), 54-66. ISSN Print: 3079-5192; ISSN Online: 3079-5206.
https://doi.org/10.63313/AERpc.9049
Published: 2025-08-29

Abstract

IN718 alloy, a typical nickel-based superalloy, is widely used in key components such as turbine blades and combustion chambers in aircraft engines due to its excellent high-temperature strength, creep resistance, and corrosion resistance. However, the material's high-temperature strength, poor thermal conductivity, and low plasticity lead to low efficiency in traditional machining and severe tool wear. Laser processing, with its high energy density, non-contact nature, and flexibility, is considered an effective method for machining micro-holes in high-temperature alloys. However, laser micro-hole processing in air still faces problems such as large hole expansion, rough hole walls, a large heat-affected zone, and thick oxide layers. To address these issues, this paper introduces a water-assisted environment and combines pulse delay technology to explore its effects and mechanisms in the micro-hole processing of IN718 alloy.

Keywords

Synergistic laser drilling, pulse-delay modulation; dynamic energy regulation; micropore processing

1. Introduction

Microporous structures play a pivotal role in aeroengine turbine blades by providing air-film cooling holes that alleviate thermal stress and improve high- temperature performance [1,2]. These holes require diameters below 1 mm and depth-to-diameter ratiosexceeding 13:1 to meet stringent cooling demands [3], and must be fabricated in hard-to-machine superalloys such as Inconel 718 [4,5].Traditional drilling methods face trade-offs: mechanical drilling and milling struggle with micron-scale precision [6], while EDM and ECM achieve fine features but introduce thermal defects or consume large electrolyte volumes, raising environmental and cost concerns [7－10].Laser drilling, by contrast, is non-contact [11] and largely material- independent [12]. At power densities above 10^{10}W/cm², ablation rates increase dramatically to support high- throughput deep-hole machining [13]. However, high- power laser drilling often induces thick recast layers and rough hole walls [14], and produces extensive heat- affected zones (HAZ) in deep holes [15]. Thermal accumulation further degrades quality [16], and polarization effects exacerbate asymmetries, leading to poor roundness and irregular exit shapes [17]. Short- pulse and ultrashort-pulse lasers can reduce ther32412mal damage but are costly and inefficient at industrial throughputs [18－20], whereas nanosecond lasers, though more economical and higher in removal rate, tend to amplify polarization-induced irregularities [21－23].Research on laser pulse delay technology for micro-hole machining in an air environment still faces challenges in avoiding processing defects. This is primarily because, as the hole depth increases, the laser beam's incident angle relative to the hole wall gradually increases, leading to a significant enhancement of the material's differential absorption of P-polarized and S-polarized light, which intensifies the asymmetric polarization absorption effect on the hole walls. This results in irregularities in the hole exit morphology. Additionally, during processing in air, a large amount of oxide layer inevitably forms on the hole walls, affecting the processing quality. Liquid-assisted technology is an effective method to overcome laser polarization effects. By introducing the processing environment into a low-oxygen liquid, it suppresses the occurrence of oxidation reactions. When the laser focuses on substances in the solution, the liquid near the solid surface undergoes superheating, generating a large number of gas bubbles. The bubble clusters, through explosive boiling and rupture, release short light pulses and shockwaves, which have a material removal and modification effect on the hole walls. However, when combined with laser pulse delay technology, the specific effects of liquid-assisted laser composite processing still need further in-depth verification.

2. Experimental details

2.1. Materials and equipment

Aerospace nickel-based alloy IN718 (20 mm × 20 mm × 1 mm) was selected for machining. Prior to the experiment, the surface was polished using a metallographic grinder and cleaned with an ultrasonic cleaner (KQ-50DE) to remove oxidation and impurities. Elemental analysis revealed high concentrations of Ni, Cr, Fe, and Nb (see **Table 1**). The chemical solution for the experiment was prepared by mixing 1 mol/L NaNO3 and 1 mol/L HCl with distilled water. All experiments were conducted under controlled conditions in a class 1000 clean room at 25° C.The micromachining system included a nanosecond laser (IPG YLPN-1-100-200-R) with a wavelength of 1064 nm, pulse width of 100 ns, power up to 200 W, and repetition frequency of 20-2000 kHz. The laser spot radius was 25 μm with a beam intensity of 5.6 kW/mm². The system consisted of a beam expander, galvanometer scanning system, and mirrors, with a scanning range of 175 mm × 175 mm. The Post-drilling, samples were rinsed with alcohol and deionized water, then dried. Laser confocal microscopy (LCM) was used to assess hole profiles and surface morphology, while scanning electron microscopy (SEM) analyzed the recast and oxide layers. Elemental compositions were determined using x-ray energy spectrometry (EDS). Experimental data represent the average of multiple measurements to minimize errors.

Table 1.1 Composition of nickel-based superalloy (IN718)

Element	Ni	Cr	Fe	Nb	Mo	Ti	Co	Cu	Si	Mn	C
Wt.%	53.66	18.41	17.9	4.92	2.87	0.96	0.34	0.13	0.09	0.08	0.03

2.2. The mechanism of pulse delay

Currently, most research focuses primarily on static laser drilling modes, with less attention given to the dynamic characteristics during the drilling process, limiting the optimization of micro-hole machining quality and efficiency. To mitigate the adverse effects of high-energy laser output, this paper proposes a laser pulse delay scanning drilling method. As shown in **Figure 2**, this method delays the laser pulses to segment the energy output, adjusting the delay time between pulse bursts to dynamically control energy release. Two delay strategies were used in the experiment: equal pulse number delay and unequal pulse number delay. In the equal pulse number delay method, a fixed delay is set between pulse groups, resulting in a regular output, while in the unequal pulse number delay method, the number of pulses per group and the delay time are adjusted to create a periodic cycling output. Unlike altering the pulse repetition frequency, the pulse delay technique precisely controls the timing of pulse energy output, ensuring the laser energy is fully utilized, thereby optimizing the interaction between the laser and the material. During the laser pulse delay scanning process, the laser scans along a concentric circular path from the outermost circle inward, introducing delay after completing each concentric ring to ensure each ring is fully processed. This avoids irregular shapes caused by improper delays. This method improves the quality of micro-hole machining and optimizes machining efficiency.

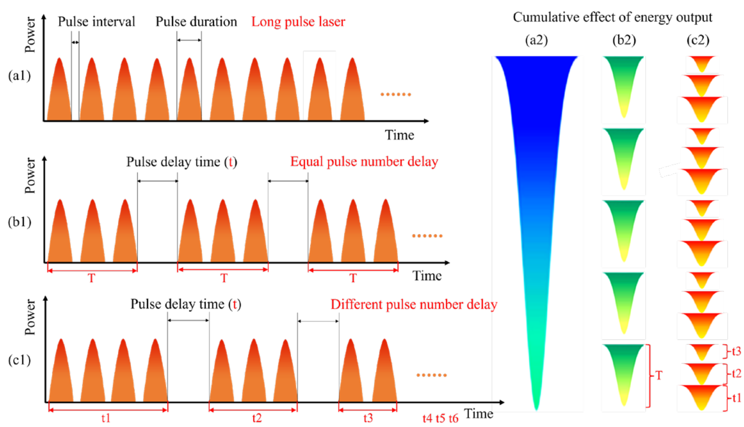

Fig. 2 Schematic diagram of laser pulse delay action principle: (a) No delay; (b) Equal pulse number delay; (c) Unequal pulse number delay; (1) Pulse output schematic diagram; (2) Energy output cumulative

3. Design of water-assisted laser pulse delay processing scheme

Flowing water generates more shockwave energy than stagnant water, making it more effective in removing debris particles inside the hole. Two dynamic water-assisted strategies were designed for the experiment, as shown in **Figure 3.1**: top-facing water-assisted and back-facing water-assisted, both including two stages: blind hole processing and through-hole processing. In the experiment, water flow is circulated through a peristaltic pump, and the flow rate is precisely controlled using a speed controller and flow meter to ensure a stable impact on the material surface. The top-facing water-assisted nozzle is positioned above the workpiece, and dynamic water flows at a certain angle and speed from top to bottom, forming a stable thin water film on the workpiece surface. The nanosecond laser passes through the water layer and then acts on the workpiece surface. Both stages quickly flush the hole wall through the impact, with the main difference being the direction of the water flow in removing the molten debris: during blind hole processing, the debris is ejected from the top, while in through-hole processing, debris is ejected from both the upper and lower surfaces. In back-facing water-assisted laser processing, the nozzle is positioned below the workpiece, and dynamic water flows at a certain speed from bottom to top, with circulating water continually present on the lower surface. Unlike top-facing water-assisted processing, during the blind hole stage, the upper surface of the workpiece is directly exposed to air, and only after the through-hole is formed does thewater flow from below into the microhole, participating in the laser composite processing.

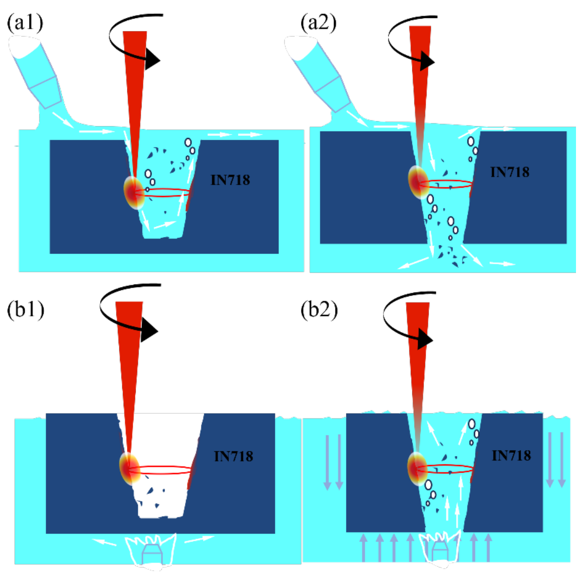

Fig. 3.1 Water-assisted processing: (a) Upward jet water assistance; (b) Backward jet water assistance; (1) First stage: blind hole processing; (2) Second stage: through hole processing

4. Effect of back-facing water-assisted laser pulse delay processing parameters

4.1. Effect of water layer position on micro-hole morphology

Liquid jets can be classified into free jet, impinging jet, and wall jet regions, with the impingement and wall jet zones being the primary areas for forced convection. The water layer position not only determines the thickness of the liquid layer and the volume of liquid entering the micro-hole, but also directly influences the plasma shockwave and cavitation effects, which affect the hole wall quality in water-assisted laser processing.

The experiment used a hole diameter of 400 μm, a filling distance of 20 μm, repetition frequency of 20 kHz, laser power of 200 W, scanning speed of 50 mm/s, 30 scanning passes, and a water flow rate of 30 L/h. The water surface was positioned 0 mm relative to the workpiece's lower surface focal plane, as shown in **Figure 4.1(a)**. The experiment explored the effect of different water layer positions on micro-hole processing, with morphology results shown in **Figure 4.1(b)**. During the second stage of back-facing water-assisted processing (through-hole processing), water enters the hole. At 0 mm water layer, less liquid enters the hole, and the oxide layer is visible. At 0.5 mm, the best removal effect is achieved, with regular hole shape. Micro-hole dimensions are shown in **Figure 4.1 (c1, c2)**, with a minimum taper of 2.06° and roundness of 95.8%. As the water layer increases and aligns with the workpiece upper surface, the taper change is minimal, but water splashing marks appear at the hole entrance, indicating explosive boiling and pressure waves during laser processing. When the water layer reaches 1.5 mm, the workpiece is submerged. Under high-power laser conditions, the water absorbs more energy, causing rapid heating and vaporization, leading to unstable processing with irregular ablation marks. The flowing water causes focal point instability, resulting in a larger micro-hole entrance and worse taper and roundness. In conclusion, the 0.5 mm focal plane position yields the best results.

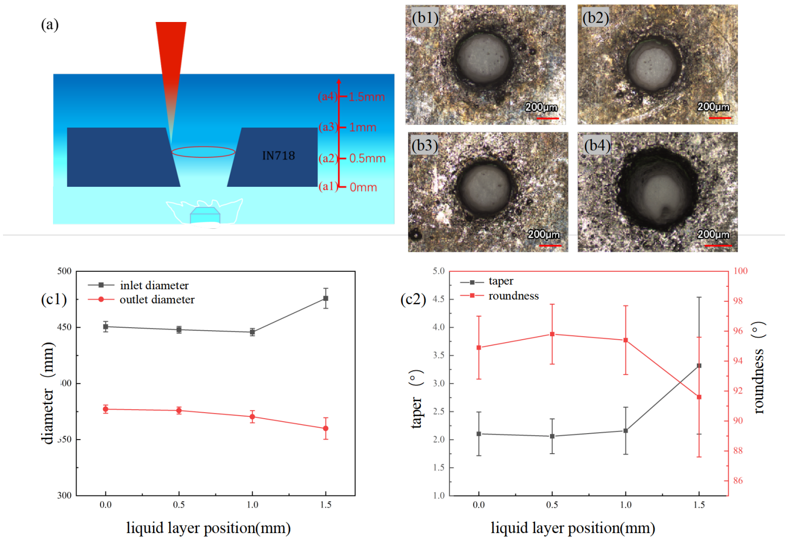

Fig. 4.1 (a) Focal plane at different liquid layer positions; (b) Micro-hole entrance morphology corresponding to different liquid layer positions; (c1) Variation trend of micro-hole diameter;(c2) Variation trend of roundness and taper

4.2. The effect of defocus amount on micro-hole morphology

Material removal is achieved through the high energy density laser heat source formed by the laser beam focused through a lens. The nanosecond laser energy exhibits a Gaussian distribution in space, with the highest energy density at the focal point after focusing. As shown in **Figure 4.2(a)**, when the laser focus is on the workpiece surface, it is defined as the focal plane, where the spot diameter is smallest and laser energy is maximal. When the laser focus moves downward and the actual focus is below the material surface, it is considered a negative defocus state, with the defocus amount being negative. When the laser focus is above the material surface, it is a positive defocus state, and the defocus amount is positive. In high-power laser processing, the refractive index of water is 1.33, but during the actual process, the initial refractive index of the liquid is greater than that of air. However, due to the presence of high-temperature and high-pressure steam or plasma layers, the refractive index of steam and plasma is smaller than that of air, which may cause further changes in the focal position. Therefore, the experiment selected a water layer position of 0.5 mm and focal plane, laser power of 200 W, 30 passes, with the defocus range varying from -1 mm to 0.5 mm. Micro-hole dimensions and morphology were compared at different focus positions.**Figure 4.2(b)** shows the experimental results. When a positive defocus of 0.5 mm is applied, the micro-hole shows a distinct conical shape with poor taper, as the laser focus is above the workpiece, and the laser energy decreases with the increasing hole depth, resulting in poor material removal on the lower half. When the defocus amount is changed from a positive 0.5 mm to a focus on the workpiece surface at 0 mm, the micro-hole exit diameter increases significantly, and the micro-hole taper shows a "transition" phenomenon with a noticeable reduction. The laser beam spot diameter changes from defocused to focused, with more energy concentrated in a smaller area, thereby improving processing accuracy and efficiency. At a defocus of -0.5 mm, when the focus is at the workpiece center, the micro-hole sidewall profile is optimal, with the minimum taper. However, as the laser focus continues to deepen, at a defocus of -1 mm, the laser focus is below the processing surface, causing the hole wall to widen. This is because the laser beam spot diffuses on the workpiece surface, resulting in a relatively low energy density per unit area, but a larger irradiated area. This increases the contact area between the laser beam and the workpiece surface during processing, causing the hole wall to widen. Additionally, negative defocus leads to less concentrated energy, and the melted material may not fully vaporize or be removed by the water flow, causing some areas of the hole wall to remelt and form irregular, wider hole walls with lower quality. Experimental results show that when the laser is focused inside the workpiece, the defocus amount near -0.5 mm yields the smallest micro-hole taper and the best results.

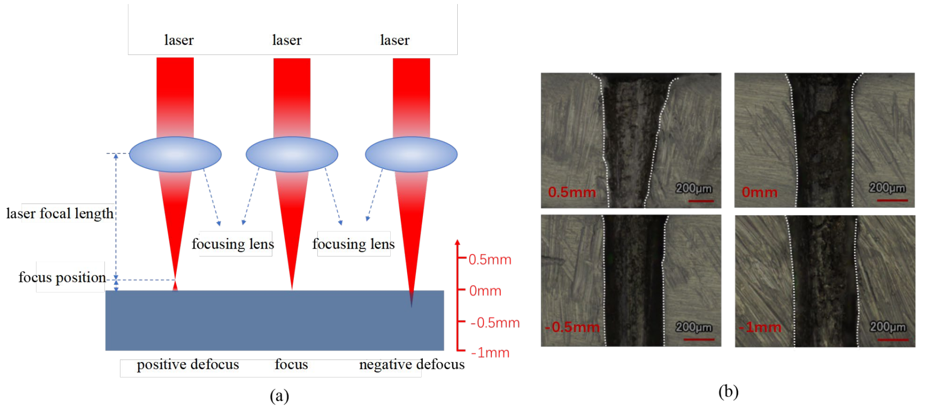

Fig. 4.2 (a) Different focal planes; (b) Micro-hole wall morphology corresponding to different focal planes

4.3. Back-facing water-assisted laser pulse delay micro-hole morphology analysis

The material removal is achieved through the high-energy density laser heat source formed by the laser beam focused through a lens. The nanosecond laser energy exhibits a Gaussian distribution in space, with the highest energy density at the focal point after focusing. As shown in **Figure 4.3(a1)**, when the back-facing water-assisted processing is performed without delay, the morphology is similar to that in air, with a significant amount of molten debris (spatter) around the hole entrance. The entrance diameter is very large, and the expansion is obvious, resembling a "bowl shape." Although no prominent recast layer like in air is observed, numerous microcracks still exist. As seen in **Figure 4.3(a2)**, intense oxidation occurs at the entrance, resulting in a high oxygen content. This phenomenon is mainly due to the lower water layer position, and during the first stage of blind hole processing with back-water method, the laser is violently output from the beginning, repeatedly treating the entrance edge with laser etching, leading to severe heat accumulation, which damages the hole morphology and cannot be completely repaired. When the through-hole is formed and enters the second stage, water quickly rushes through the exit, triggering a new material removal mechanism. The hole walls and entrance experience strong cooling, creating local thermal stress and generating many microcracks. Additionally, due to the capillary effect, the water flowing out of the micro-hole entrance carries some laser energy, thus increasing the material removal rate at the entrance.

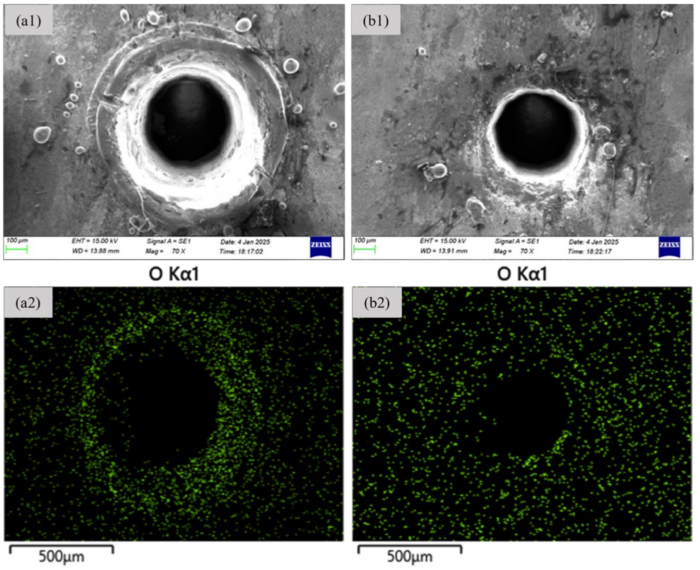

Fig. 4.3 (a) Backward jet water assistance without delay; (b) Backward jet water assistance with delay; (1) SEM image of micro-hole entrance morphology; (2) Oxygen element distribution map

Using pulse delay, as shown in **Figure 4.3(b1)**, intermittent energy output is achieved from the beginning, controlling the processing intensity. The expansion of the micro-hole entrance is minimal, and the hole diameter is well controlled. As the through-hole forms, the laser energy distribution becomes more uniform under the high thermal conductivity of water, and the recast layer is cleared again. The amount of spatter is controlled and significantly reduced, leading to a more uniform hole wall surface with fewer microcracks, significantly improving the hole wall quality. As shown in **Figure 4.3(b2)**, the oxygen content at the entrance is extremely low, and the thin liquid film formed on the material surface helps suppress high-temperature oxidation, preventing the formation of excessive oxides.

The experiment compared the micro-hole wall morphology when back-facing water-assisted laser processing was done with and without pulse delay. Without delay, as shown in **Figure 4.4(a1-d1)**, the hole walls exhibited numerous etched pits caused by cavitation bubble collapse, irregular recast layers, many microcracks, and re-deposition of ablation debris and re-solidified micro-particles on the surface. The analysis shows that concentrated laser energy acting on the same area induces cavitation bubbles, suspended debris, and light scattering caused by turbulent liquid, reducing the stability of laser beam transmission. The boiling phenomenon generates large-scale bubbles, and the bubbles cause a "shielding" effect on the laser, resulting in diffraction phenomena. As the scanning continues, the bubble volume increases, and when it reaches a certain size, strong scattering occurs at the center-top of the bubble. This leads to very low processing efficiency, and strong diffraction near the edges causes deflection in the laser's processing direction, resulting in uneven etching on the hole wall. Furthermore, when the bubbles collapse, they release high-intensity shockwaves, generating micro-jets that impact the molten or semi-solid material on the hole wall, accelerating local material removal and forming small etching pits. The larger the bubble, the stronger the impact force upon collapse, leading to deeper and more noticeable etching pits. The presence of flowing liquid also causes the molten material to solidify in a dynamic environment, resulting in irregular shapes. Pulse delay indirectly controls the laser repetition frequency, suppressing the formation of large bubbles. The hole wall morphology shown in **Figure 4.4(a2-d2)** displays only a few etching pits at the upper end of the micro-hole, with the rest of the hole wall having low roughness, and the molten surface is relatively smooth. This is because the material melts, vaporizes, and explosively generates gas flow in a very short time. After each delayed pulse burst, the backpressure is very strong, and the vaporized and melted material is rapidly ejected, increasing the splattering content. The existence of delay time also reduces the temperature gradient between the base material and the molten material, reducing the generation of microcracks in the weaker areas between dendrites. Pulse delay also decreases secondary deposition of the molten material. Before the plasma expands, the laser irradiation has stopped, allowing dissipation of plasma and debris, improving the quality of micro-hole processing.

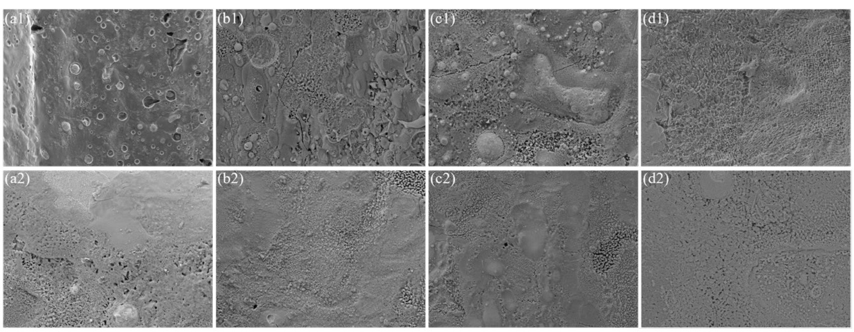

Fig. 4.4 Micro-hole wall morphology: (1) Backward jet water assistance without delay; (2) Backward jet water assistance with delay; (a) Upper part; (b) Middle part; (c) Lower part; (d) Bottommost part

The introduction of water flow further reduced the taper of the micro-hole, improved the roundness, reduced the heat-affected zone, and enhanced the micro-hole morphology. **Figures 4.5(a1, b1)** show a comparison of micro-hole morphology with pulse delay in air and back-facing water-assisted processing. To better distinguish the recast layer and other remelted areas from the base material, a corrosion solution was prepared by mixing anhydrous copper sulfate and hydrochloric acid in alcohol. The polished hole wall was immersed in the chemical solution for 3 minutes, followed by ultrasonic cleaning in alcohol. This chemical metallographic etching revealed the recast layer region on the metal surface. This method does not remove the oxide layer but exposes the appearance of the base material. As shown in **Figures 4.5(a2, b2, a3, b3)**, the recast layer thickness of the micro-hole was significantly improved under the influence of water assistance, and the area layering was not apparent. Energy dispersive spectroscopy (EDS) was then used to analyze the surface morphology, elemental distribution, and content of different recast layer regions. In air, the recast layer had a higher oxygen content, concentrated near the hole wall, while in the water-assisted element map, the oxygen content was very low. The presence of water suppressed the oxidation reaction, reducing the recast layer thickness.Further analysis of the back-facing water-assisted pulse delay processing was performed at the hole wall positions (points A and B in **Figure 4.5**) to measure the elemental content. The results, shown in **Figures 4.5(c, d)**, indicate that the water-assisted surface showed signs of incomplete removal. Some areas on the inner hole wall still retained the unremoved oxide layer, particularly near the upper end of the micro-hole, which is closer to the air, where full suppression could not be achieved. However, at the lower end of the micro-hole, the oxygen content was extremely low. This is closely related to the water layer position and the jet direction; the oxygen from the air could not penetrate deeply at the lower end of the hole, making the hole wall relatively uniform without the presence of the oxide layer. To address this defect, further removal should be considered.

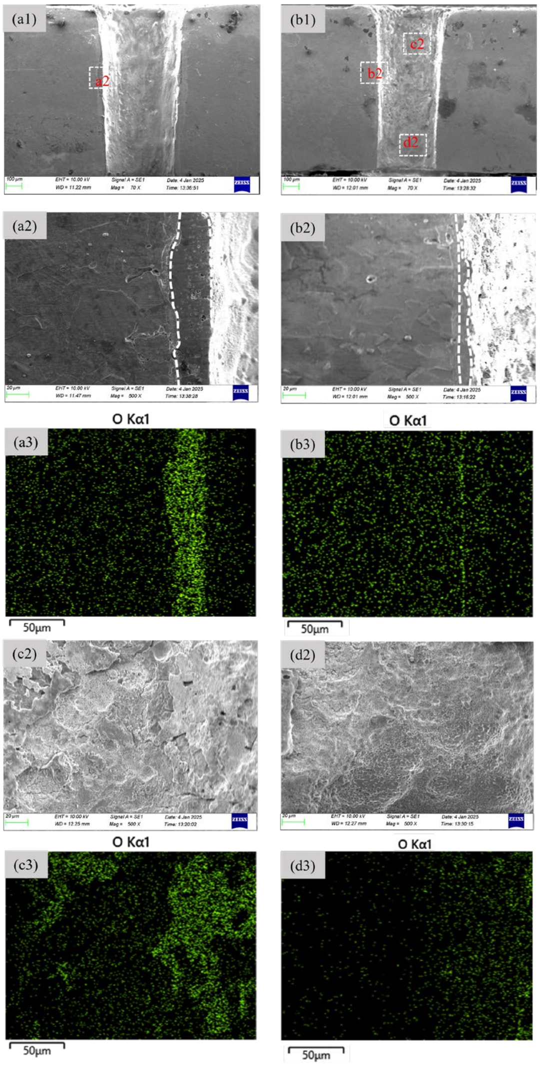

Fig 4. 5 Micro-hole wall morphology analysis after metallographic etching: (a) Pulse delay in air; (b-d) Pulse delay with backward jet water assistance; (1) Overall view of the hole wall; (2) Local magnified image; (3) Oxygen element distribution map

5. Conclusion

This study proposes a water-assisted laser processing technology and develops two water-assisted processing schemes: top-facing water-assisted and back-facing water-assisted. Both schemes were tested with and without pulse line delay, and a comparative analysis was conducted to determine the optimal scheme. The effects of ablation threshold, water layer position, and defocus amount on back-facing water-assisted laser pulse delay drilling were explored. The orthogonal experimental method was used to optimize the process parameters, ultimately achieving the best micro-hole morphology. The main research findings are as follows: The micro-hole morphology obtained from back-facing water-assisted pulse delay processing exhibited the best hole entrance shape, with no obvious recast layer, spatter, or other defects. The oxygen content at the entrance was significantly reduced, the hole wall was smooth, and the roughness was low. The pulse delay mechanism reduced the temperature gradient between the substrate and the molten material, thus decreasing the possibility of microcracks in the weaker areas between dendrites. Additionally, this strategy reduced the secondary deposition of the molten material, as laser irradiation ceased before plasma expansion, allowing the plasma and debris to dissipate, which reduced the recast layer thickness and improved the micro-hole processing quality. However, a portion of the oxide layer remained at the upper end of the micro-hole, while the oxide layer at the lower end was almost completely removed.

Acknowledgements

This work was support by 111 project of China [D21017]; Shandong Provincial Key Research and Development Program (International Science and Technology Cooperation) [No.2024KJHZ002]; Natural Science Foundation of Shandong Province [No. ZR2023ME156]; "Double Hundred Plan" Talent Program of Shandong Province [WSR2023055]; National Natural Science Foundation of China [52405492]; Qingdao Natural Science Foundation [25- 1-1-207-zyyd-jch].

References

[1] Zhao W， Yu Z （2018） Self-cleaning effect in high quality percussion ablating of cooling hole by picosecond ultra-short pulse laser. Opt Lasers Eng 105:125 – 131. https://doi.org/10.1016/j.optlaseng.2018.01.011

[2] Gurav MM, Gupta U, Dabade UA (2019) Quality evaluation of precision micro holes drilled using pulsed Nd: YAG laser on aerospace nickel-based superalloy. Mater Today: roc 19:575-582. https://doi.org/10.1016/j.matpr.2019.07.736

[3] Zhang F, Wang J, Wang X, Zhang J, Hayasaki Y, Kim D, Sun S (2021) Experimental study of nickel- based superalloy IN792 with femtosecond laser drilling method. Opt Laser Technol 143:107335. https://doi.org/10.1016/j.optlastec.2021.107335

[4] Mishra S, Yadava V (2013) Modeling and optimization of laser beam percussion drilling of nickel-based superalloy sheet using Nd: YAG laser. Opt Lasers Eng 51(6):681-695. https://doi.org/10.1016/j.optlaseng.2013.01.006

[5] Sen M, Shan HS (2005) A review of electrochemical macro-to micro-hole drilling processes. Int J Mach Tools Manuf 45(2):137-152. https://doi.org/10.1016/j.ijmachtools.2004.08.005

[6] Chen G, Xu J, Lian Z, Wang J, Li Y, Wang J, Yu H (2021) Study on the amplitude effect on micro-hole drilling of AISI 4340 by ultrasonic vibration. Int J Adv Manuf Technol 116:2437-2453. https://doi.org/10.1007/s00170-021-07617-y

[7] Pereira RB, Brandão LC, de Paiva AP, Ferreira JR, Davim JP (2017) A review of helical milling process. Int J Mach Tools Manuf 120:27-48. https://doi.org/10.1016/j.ijmachtools.2017.05.002

[8] Yeo CY, Tam SC, Jana S, Lau MW (1994) A technical review of the laser drilling of aerospace materials. J Mater Process Technol 42:15-49. https://doi.org/10.1016/0924-0136（94）90073-6

[9] Mao X, Almeida S, Mo J, Ding S (2022) The state of the art of electrical discharge drilling: A review. Int J Adv Manuf Technol 121:2947-2969.

https://doi.org/10.1007/s00170-022-09549-7

[10] Fang XL, Wang XD, Wang W, Qu NS, Li HS (2017) Electrochemical drilling of multiple small holes with optimized electrolyte dividing manifolds. J Mater Process Technol 247:40 – 47. https://doi.org/10.1016/j.jmatprotec.2017.04.013

[11] Li Q, Yang L, Hou C, Adeyemi O, Chen C, Wang Y (2019) Surface ablation properties and morphology evolution of K24 nickel based superalloy with femtosecond laser percussion drilling. Opt Lasers Eng 114:22-30. https://doi.org/10.1016/j.optlaseng.2018.10.010

[12] Zhang R, Li W, Liu Y, Wang C, Wang J, Yang X, Cheng L (2015) Machining parameter optimization of C/SiC composites using high power picosecond laser. Appl Surf Sci 330:321-331. https://doi.org/10.1016/j.apsusc.2015.01.010

[13] Duan W, Mei X, Fan Z, Li J, Wang K, Zhang Y (2020) Electrochemical corrosion assisted laser drilling of micro-hole without recast layer. Opt 202:163577. https://doi.org/10.1016/j.ijleo.2019.163577

[14] Chien WT, Hou SC (2007) Investigating the recast layer formed during the laser trepan drilling of Inconel 718 using the Taguchi method. Int J Adv Manuf Technol 33:308 – 316. https://doi.org/10.1007/s00170-006-0454-1

[15] Beck T (2011) Laser drilling in gas turbine blades: Shaping of holes in ceramic and metallic coatings. Laser Technik Journal, 8(3):40-43. https://doi.org/10.1002/latj.201190024

[16] Hsu JC, Lin WY, Chang YJ, Ho CC, Kuo CL (2015) Continuous-wave laser drilling assisted by intermittent gas jets. Int J Adv Manuf Technol 79:449 – 459. https://doi.org/10.1007/s00170-015-6847-2

[17] Li ZY, Wei XT, Guo YB, Sealy MP (2015) State- of-art, challenges, and outlook on manufacturing of cooling holes for turbine blades. Mater Sci Technol 19(3):361-399. https://doi.org/10.1080/10910344.2015.1051543

[18] Zhai Z, Wang W, Mei X (2017) Simulation and experimental study on laser drilling of nickel-based alloy with thermal barrier coatings. Int J Adv Manuf Technol 90:1871-1879. https://doi.org/10.1007/s00170- 016-9485-4

[19] Yang Z, Ji P, Zhang Z, Ju Y, Wang Z, Zhang Q, Wang C, Xu W (2020) Fundamental 3D simulation of the femtosecond laser ablation for cooling hole drilling on Ni and Fe based aero-engine components. Opt Commun 475:126237. https://doi.org/10.1016/j.optcom.2020.126237

[20] Jiang H, Ma C, Li M, Cao Z (2021) Femtosecond laser drilling of cylindrical holes for carbon fiber- reinforced polymer (CFRP) composites. Mol 26:2953. https://doi.org/10.3390/molecules26102953

[21] Perrie W, Rushton A, Gill M, Fox P, O'Neill W (2005) Femtosecond laser micro-structuring of alumina ceramic. Appl Surf Sci 248(1-4):213-7. https://doi.org/10.1016/j.apsusc.2005.03.005

[22] Zhang T, Yuan H, Cai M (2023) Effects of recast layer on fatigue performance of laser-drilled holes in nickel-based superalloy. J Mater Process Technol 311:117821. https://doi.org/10.1016/j.jmatprotec.2022.117821

[23] Weber R, Michalowski A, Abdou-Ahmed M, Onuseit V, Rominger V, Kraus M, Graf T (2011) Effects of radial and tangential polarization in laser material processing. Phys Procedia 12:21-30. https://doi.org/10.1016/j.phpro.2011.03.004.